Journal of Sound and Vibration (2000) **235**(5), 787–800
doi:10.1006/jsvi.2000.2958, available online at http://www.idealibrary.com on IDEAL®

ACTIVE CANCELLATION OF NOISE IN A CAR CABIN USING THE ZERO SPILLOVER CONTROLLER

MINGSIAN R. BAI AND HSIUHONG CHEN

Department of Mechanical Engineering, National Chiao-Tung University, 1001 *Ta-Hsueh Rd., Hsin-Chu, Taiwan, Republic of China*

(*Received* 6 *December* 1999, *and in final form* 8 *February* 2000)

In active noise control problems, spillover will occur because of the Bode integral constraint if the performance sensors and measurement sensors are collocated, or if the control speakers and the noise sources are collocate. This paper is focused on the implementation of a multiple-channel zero-spillover ANC controller using a spatially feedforward structure for a car cabin. The plant model is realized by using a frequency-domain procedure. The linear-quadratic-Gaussian algorithm is used in controller design. Experiments are carried out to verify the proposed technique, where random noise and engine noise are chosen as the primary noise. The results indicate that the proposed controller yields a broadband attenuation for the random noise. The proposed method is also effective in attenuating the engine noise if an assumed model of the noise is incorporated into controller design.

1. INTRODUCTION

Since Paul Lueg proposed the idea of active noise control (ANC) in 1936, the technique has received considerable research attention. In viewing the ANC development to date, the control structures generally fall into three categories: feedforward structure, feedback structure and hybrid structure. The choice of control structures depends on the nature of the problem, such as the availability of non-acoustical reference, problem size and bandwidth. If non-acoustical signals of the disturbance are measurable, either feedforward structure or hybrid structure will be effective [1]. If non-acoustical reference is unavailable but the problem size is small, e.g., active headsets, conventional feedback control is still a viable approach [2]. On the other hand, if the problem size is not small, e.g., a three-dimensional enclosure, direct application of feedback control can generally achieve only narrowband attenuation [3]. This is a typical problem that frequently occurs to conventional feedback structure, where the performance sensors and measurement sensors are collocated, or the control speakers and the noise sources are collocated. The so-called *spillover* problem will arise because of the Bode integral constraint [4]. When non-acoustical reference is not accessible, the spatially feedforward structure has widely been used as an alternative. An acoustical sensor has to be placed upstream near the primary source. It is also pointed out in an excellent theoretical investigation by Hong and Bernstein [4] that the spatially feedforward structure does not suffer from spillover problem so much as conventional feedback control, provided the measurement sensor (near the noise source) and the performance sensor are not collocated, the noise source and the control speaker (near the performance sensor) are also not collocated. The duct ANC system is shown in Figure 1(a)

0022-460X/00/350787 + 14 $35.00/0

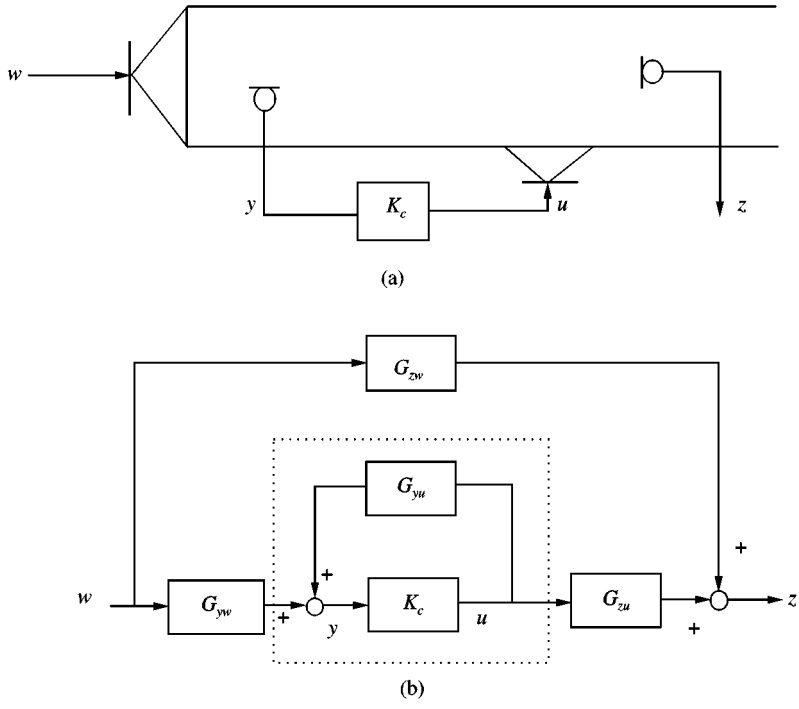

Figure 1. The duct ANC problem: (a) the arrangement of sensors and speakers; (b) the block diagram.

as an example of the spatially feedforward structure, where **w**, **u**, **y**, and **z** are disturbance input, control input, measurement output and performance output respectively. The transfer function $\mathbf{K}_c$ denotes the spatially feedforward controller. The ANC system is also represented in the block diagram of Figure 1(b) and the transfer functions G_{yw}, G_{yu}, G_{zw} and G_{zu} denote the paths from each speaker to each sensor.

It is remarked that the term *spatially feedforward* only means the measurement sensor is geometrically very close to the noise source. The control structure is still feedback in nature because the measurement sensor measures the system response (the primary noise and the acoustic feedback) at the upstream position, and not directly the excitation input. It is also this acoustic feedback that results in severe degradation of performance and stability in ANC systems, as opposed to the feedforward structure and the hybrid structure.

The contribution of this paper is primarily on the actual implementation of a multiple-channel zero-spillover (ZSP) controller using spatially feedforward structure. In particular, augmented plant realization using frequency-domain identification and assumed disturbance model are two crucial steps among the implementation aspects. The development is essentially a continuation of the theoretical and numerical work by Hong and Bernstein [4]. The targeted application is an active attenuation of the noise in a car cabin. Because an ideal ZSP controller is generally improper and thus not implementable, the linear-quadratic-Gaussian (LQG) control is employed for obtaining an approximate ZSP controller. In addition, the original version of the ZSP controller proposed by Hong and Bernstein requires the dynamics from the noise source to the measurement sensor and performance sensor be known *a priori*. This poses a problem in practical applications, where the noise source is not measurable by any non-acoustical means. To circumvent this problem, an assumed model of the noise dynamics is incorporated into controller design.

The mathematical model of an augmented plant is determined using a frequency-domain procedure. Then an optimal controller is designed using LQG synthesis and implemented on a digital signal processor. Practical considerations during implementation are addressed. Broadband random noise and engine exhaust noise are chosen in experiments to demonstrate the effectiveness of the spatially feedforward ZSP controller.

2. IDEAL ZERO SPILLOVER CONTROLLER

In this section, a multiple-input–multiple-output (MIMO) ZSP controller using spatially feedforward structure is formulated. The controller is a MIMO extension of the ZSP controller proposed by Hong and Bernstein [4]. The details of the Bode integral constraints and the rationale of the single-input/single-output (SISO) ZSP controller can be found in the original paper and are thus omitted here.

First, the ANC problem using spatially feedforward structure can be expressed in terms of the generalized control framework containing an augmented plant $\mathbf{G}(z)$ and a controller $\mathbf{K}_c(z)$, as shown in Figure 2. The augmented plant $\mathbf{G}(z)$ can further be partitioned into four submatrices $\mathbf{G}_{yw}(z)$, $\mathbf{G}_{zw}(z)$, $\mathbf{G}_{yu}(z)$, and $\mathbf{G}_{zu}(z)$, with the meanings self-explanatory in the subscripts. Hence, the input–output relationship of the plant and the controller can be expressed as

$$\begin{bmatrix} z \\ y \end{bmatrix} = \begin{bmatrix} G_{zw}(z) & G_{zu}(z) \\ G_{yw}(z) & G_{yu}(z) \end{bmatrix} \begin{bmatrix} w \\ u \end{bmatrix} \tag{1}$$

and

$$\mathbf{u} = \mathbf{K}_c(z)\mathbf{y}. \tag{2}$$

The closed-loop transfer function from $\mathbf{w}$ to $\mathbf{z}$ can be written as

$$\mathbf{z} = \mathbf{T}_{zw}(z)\mathbf{w}, \tag{3}$$

where

$$\mathbf{T}_{zw}(z) = [\mathbf{G}_{zw}(z) + \mathbf{G}_{zu}(z)\mathbf{K}_c(z)(\mathbf{I} - \mathbf{G}_{yu}(z)\mathbf{K}_c(z))^{-1}\mathbf{G}_{yw}(z)]. \tag{4}$$

An ideal ZSP controller for perfect cancellation can be obtained by setting

$$\mathbf{T}_{zw}(z) = \mathbf{0}. \tag{5}$$

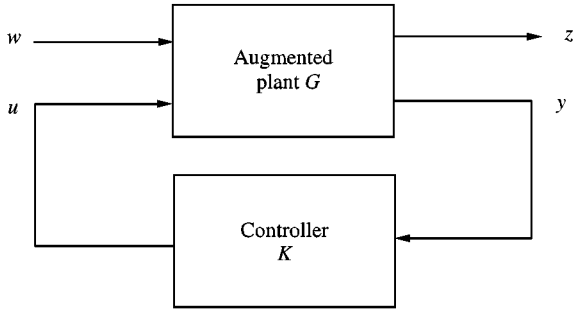

Figure 2. Generalized control framework.

The resulting controller is thus given by

$$\mathbf{K}_c(z) = (\mathbf{G}_{yu}(z) - \mathbf{G}_{yw}(z)\mathbf{G}_{zw}^{-1}(z)\mathbf{G}_{zu}(z))^{-1}. \tag{6}$$

In general, this ideal controller is improper and not implementable. To overcome the difficulty, we shall formulate in the following section an approximate ZSP controller on the basis of optimal LQG control.

3. FREQUENCY-DOMAIN SYSTEM REALIZATION AND LQG SYNTHESIS

In the synthesis of the LQG controller, a frequency-domain identification method [5] is exploited in this paper for obtaining the MIMO realization of the system. There are three practical reasons for using the frequency-domain approach. First, the signal analyzer we used in the research had only two channels. Second, this method gives a state-space realization under the MIMO framework (with common system matrices). Third, any frequency-domain weighting can be easily incorporated into the augmented plant. The procedure is briefly described as follows.

Consider the transfer function $G(z_k)$ of left matrix fraction

$$G(z_k) = Q^{-1}(z_k)R(z_k), \tag{7}$$

where

$$Q(z_k) = I_m + Q_1 z_k^{-1} + \cdots + Q_p z_k^{-p}, \tag{8}$$

$$R(z_k) = R_0 + R_1 z_k^{-1} + \cdots + R_p z_k^{-p}, \tag{9}$$

are matrix polynomials with $\mathbf{I}_m$ being an identity matrix of order m and $z_k = e^{j2\pi k/l}$, $k = 1, 2, \ldots, l$. Every $\mathbf{Q}_i$ is a $m \times m$ real square matrix and each $\mathbf{R}_i$ is a $m \times r$ real rectangular matrix. The frequency-domain identification problem can be written in a parameter equation as

$$\mathbf{\Psi} = \mathbf{\Phi}\mathbf{\Theta}, \tag{10}$$

where

$$\mathbf{\Theta} = [-Q_1 \ \cdots \ -Q_p \ R_0 \ \cdots \ R_p], \tag{11}$$

$$\mathbf{\Psi} = [G(z_0) \ G(z_1) \ \cdots \ G(z_{l-1})], \tag{12}$$

$$\mathbf{\Phi} = \begin{bmatrix} G(z_0)z_0^{-1} & G(z_1)z_1^{-1} & \cdots & G(z_{l-1})z_{l-1}^{-1} \\ \vdots & \vdots & \ddots & \vdots \\ G(z_0)z_0^{-p} & G(z_1)z_1^{-p} & \cdots & G(z_{l-1})z_{l-1}^{-p} \\ \mathbf{I}_r & \mathbf{I}_r & \mathbf{I}_r & \mathbf{I}_r \\ z_0^{-1}\mathbf{I}_r & z_1^{-1}\mathbf{I}_r & \cdots & z_{l-1}^{-1}\mathbf{I}_r \\ \cdots & \cdots & \ddots & \vdots \\ z_0^{-p}\mathbf{I}_r & z_1^{-p}\mathbf{I}_r & \cdots & z_{l-1}^{-p}\mathbf{I}_r \end{bmatrix}. \tag{13}$$

Note that $\mathbf{\Phi}$ is a $((m+r)p+r)\times(r\times l)$ data matrix, $\mathbf{\Theta}$ a $m\times((m+r)p+r)$ parameter matrix and $\mathbf{\Psi}$ a $m\times(r\times l)$ matrix. The least-squares solution of the parameter matrix $\mathbf{\Theta}$ is

$$\hat{\mathbf{\Theta}} = \begin{bmatrix} real(\mathbf{\Phi}) \\ imag[\mathbf{\Phi}] \end{bmatrix}^{+} \begin{bmatrix} real(\mathbf{\Psi}) \\ imag[\mathbf{\Psi}] \end{bmatrix}, \tag{14}$$

where "$^{+}$" denotes pseudo-inverse and "$\hat{}$" indicates the estimated value. Partitioning the matrices into the real part and the imaginary part is just to avoid complex solution.

In light of the system parameters obtained in the above identification procedure, one is ready to calculate an observable state-space realization of the MIMO system as

$$\mathbf{x}(z_k)z_k = \mathbf{A}\mathbf{x}(z_k) + \mathbf{B}\mathbf{u}(z_k), \qquad \mathbf{y}(z_k) = \mathbf{C}\mathbf{x}(z_k) + \mathbf{D}\mathbf{u}(z_k), \tag{15,16}$$

where

$$\mathbf{x}(z_k) = \begin{bmatrix} x_1(z_k) \\ x_2(z_k) \\ x_3(z_k) \\ \vdots \\ x_{p-1}(z_k) \\ x_p(z_k) \end{bmatrix}, \tag{17}$$

$$\mathbf{A} = \begin{bmatrix} \mathbf{0} & \mathbf{0} & \mathbf{0} & \cdots & \mathbf{0} & -\bar{\mathbf{Q}}_p \\ \mathbf{I}_m & \mathbf{0} & \mathbf{0} & \cdots & \mathbf{0} & -\bar{\mathbf{Q}}_{p-1} \\ \mathbf{0} & \mathbf{I}_m & \mathbf{0} & \cdots & \mathbf{0} & -\bar{\mathbf{Q}}_{p-2} \\ \mathbf{0} & \mathbf{0} & \mathbf{0} & \ddots & \mathbf{0} & \vdots \\ \mathbf{0} & \mathbf{0} & \mathbf{0} & \cdots & \mathbf{0} & -\bar{\mathbf{Q}}_2 \\ \mathbf{0} & \mathbf{0} & \mathbf{0} & \cdots & \mathbf{I}_m & -\bar{\mathbf{Q}}_1 \end{bmatrix}, \tag{18}$$

$$\mathbf{B} = \begin{bmatrix} \bar{\mathbf{R}}_p - \bar{\mathbf{Q}}_p\mathbf{D} \\ \bar{\mathbf{R}}_{p-1} - \bar{\mathbf{Q}}_{p-1}\mathbf{D} \\ \bar{\mathbf{R}}_{p-2} - \bar{\mathbf{Q}}_{p-2}\mathbf{D} \\ \vdots \\ \bar{\mathbf{R}}_2 - \bar{\mathbf{Q}}_2\mathbf{D} \\ \bar{\mathbf{R}}_1 - \bar{\mathbf{Q}}_1\mathbf{D} \end{bmatrix}, \tag{19}$$

$$\mathbf{C} = [\mathbf{0}\ \mathbf{0}\ \mathbf{0}\ \mathbf{0}\ \mathbf{0}\ \mathbf{I}_m] \tag{20}$$

and $\mathbf{D}$ is set to be $\mathbf{0}$ for strictly proper systems.

Having obtained system realization in terms of matrices $\mathbf{A}$, $\mathbf{B}$, $\mathbf{C}$ and $\mathbf{D}$, we are in a position to calculate the approximate ZSP controller using the LQG synthesis [6, 7]. In the sequel, a LQG controller will be derived in terms of a generalized system framework. We

first augment the dynamic equations as

$$\mathbf{x}(k+1) = \mathbf{A}\mathbf{x}(k) + \mathbf{B}\mathbf{u}(k) + \mathbf{D}_1\mathbf{w}(k), \tag{21}$$

$$\mathbf{y}(k) = \mathbf{C}\mathbf{x}(k) + \mathbf{D}_2\mathbf{v}(k), \qquad \mathbf{z}(k) = \mathbf{E}_1\mathbf{x}(k), \tag{22,23}$$

where $\mathbf{v}(k)$ is the sensor noise, $\mathbf{D}_1$ is the intensity of $\mathbf{w}(k)$ and $\mathbf{D}_2$ is the intensity of process noise $\mathbf{v}(k)$. For this problem, the performance output can be chosen as

$$\mathbf{z}(k) = \mathbf{E}_1\mathbf{x}(k) + \mathbf{E}_2\mathbf{u}(k), \tag{24}$$

where $\mathbf{E}_2$ is a weighting matrix for $\mathbf{u}(k)$. The significance of $\mathbf{E}_2$ lies in that it provides certain degree of robustness on account of system uncertainties and perturbations. A quadratic cost function simply reads

$$\begin{aligned} J &= \frac{1}{2}\sum_k \mathbf{z}^{\mathrm{T}}(k)\mathbf{z}(k) \\ &= \frac{1}{2}\sum_k (\mathbf{x}^{\mathrm{T}}(k)\mathbf{E}_1^{\mathrm{T}}\mathbf{E}_1\mathbf{x}(k) + 2\mathbf{u}^{\mathrm{T}}(k)\mathbf{E}_2^{\mathrm{T}}\mathbf{E}_1\mathbf{x}(k) + \mathbf{u}^{\mathrm{T}}(k)\mathbf{E}_2^{\mathrm{T}}\mathbf{E}_2\mathbf{u}(k)). \end{aligned} \tag{25}$$

The LQG synthesis includes the design of a state feedback module and a Kalman filter-based observer. These two modules can be designed independently according to the separation principle [6]. In the regulation problem, the goal is to choose a feedback gain $\mathbf{K}$ to minimize the above performance index subject to the constraint of system dynamic equation. This requires solving an algebraic Riccati equation for $\mathbf{P}_1$,

$$0 = (\mathbf{A} - \mathbf{B}\mathbf{R}_2^{-1}\mathbf{R}_{12}^{\mathrm{T}})\mathbf{P}_1 + \mathbf{P}_1(\mathbf{A} - \mathbf{B}\mathbf{R}_2^{-1}\mathbf{R}_{12}^{\mathrm{T}}) - \mathbf{P}_1\mathbf{B}\mathbf{R}_2^{-1}\mathbf{B}^{\mathrm{T}}\mathbf{P}_1 + \mathbf{R}_1 + \mathbf{R}_{12}\mathbf{R}_2^{-1}\mathbf{R}_{12}^{\mathrm{T}}. \tag{26}$$

The feedback gain $\mathbf{K}$ can then be calculated as

$$\mathbf{K} = \mathbf{R}_2^{-1}\mathbf{R}_{12} + \mathbf{R}_2^{-1}\mathbf{B}^{\mathrm{T}}\mathbf{P}_1, \tag{27}$$

where $\mathbf{R}_1 = \mathbf{E}_1^{\mathrm{T}}\mathbf{E}_1$, $\mathbf{R}_{12} = \mathbf{E}_1^{\mathrm{T}}\mathbf{E}_2$, $\mathbf{R}_2 = \mathbf{E}_2^{\mathrm{T}}\mathbf{E}_2$.

On the other hand, another algebraic Riccati equation needs to be solved for $\mathbf{P}_2$ in obtaining the Kalman observer

$$0 = (\mathbf{A} - \mathbf{V}_{12}\mathbf{V}_2^{-1}\mathbf{C})\mathbf{P}_2 + \mathbf{P}_2(\mathbf{A} - \mathbf{V}_{12}\mathbf{V}_2^{-1}\mathbf{C})^{\mathrm{T}} - \mathbf{P}_2\mathbf{C}^{\mathrm{T}}\mathbf{V}_2^{-1}\mathbf{P}_2 + \mathbf{V}_1 - \mathbf{V}_{12}\mathbf{V}_2^{-1}\mathbf{V}_{12}^{\mathrm{T}}. \tag{28}$$

The observer gain $\mathbf{L}$ can then be calculated as

$$\mathbf{L} = \mathbf{A}\mathbf{P}_2\mathbf{C}^{\mathrm{T}}(\mathbf{C}\mathbf{P}_2\mathbf{C}^{\mathrm{T}} + \mathbf{V}_2)^{-1}, \tag{29}$$

where $\mathbf{V}_1 = \mathbf{D}_1\mathbf{D}_1^{\mathrm{T}}$, $\mathbf{V}_{12} = \mathbf{D}_1\mathbf{D}_2^{\mathrm{T}}$, $\mathbf{V}_2 = \mathbf{D}_2\mathbf{D}_2^{\mathrm{T}}$. Combining the state feedback and the observer yields the resulting LQG controller

$$\mathbf{A}_C = \mathbf{A} + \mathbf{B}\mathbf{C}_C - \mathbf{B}_C\mathbf{C}, \qquad \mathbf{B}_C = (\mathbf{P}_2\mathbf{C}^{\mathrm{T}} + \mathbf{V}_{12})\mathbf{V}_2^{-1}, \qquad \mathbf{C}_C = -\mathbf{R}_2^{-1}(\mathbf{B}^{\mathrm{T}}\mathbf{P}_1 + \mathbf{R}_{12}^{\mathrm{T}}). \tag{30}$$

This concludes the LQG derivations for the generalized control framework.

4. EXPERIMENTAL INVESTIGATIONS

Experiments were conducted to evaluate the proposed ANC system. A half plywood model of a car cabin is employed in the investigation. Figure 3 shows the experimental

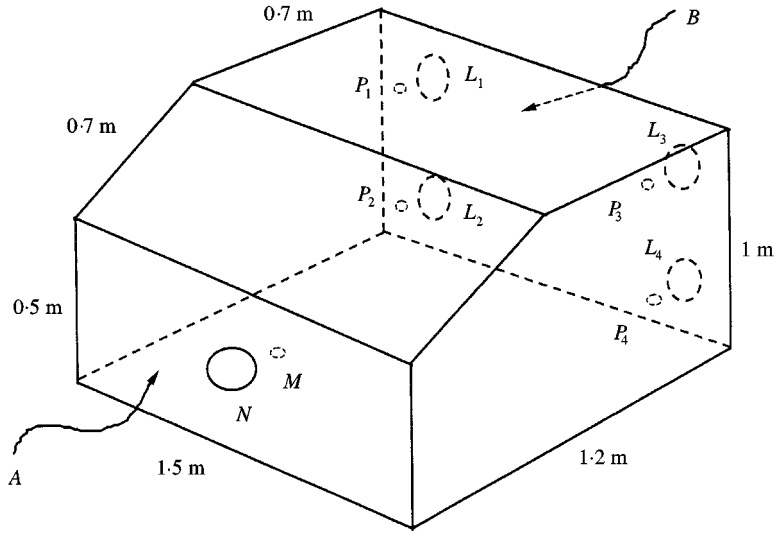

Figure 3. Half plywood model of a car cabin used in the experiments: N: primary noise speaker, M: measurement sensor, P: performance sensor, L: control speaker.

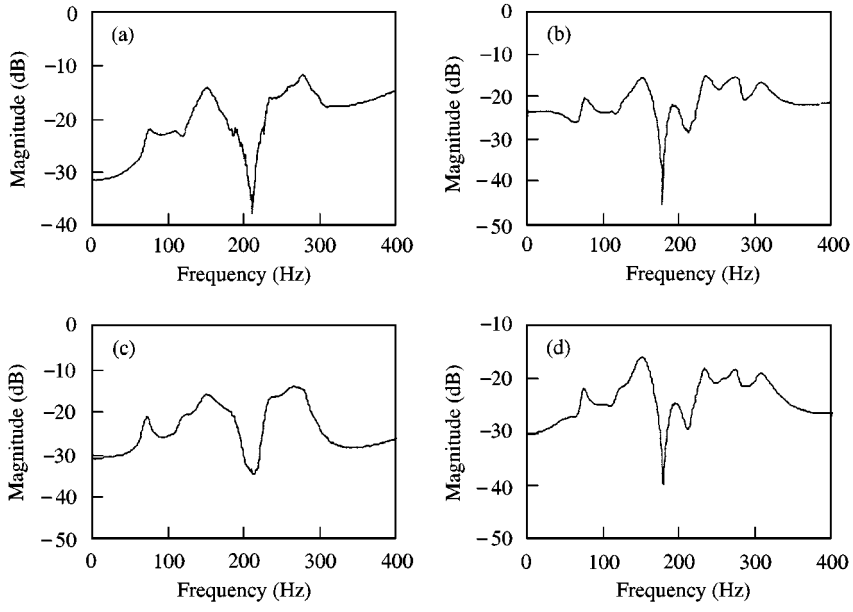

Figure 4. The models from the primary source to the performance sensors identified by the frequency-domain procedure: (a) primary source to performance sensor 1; (b) primary source to performance sensor 2; (c) primary source to performance sensor 3; (d) primary source to performance sensor 4.

arrangement. The primary noise source is mounted at the center of the plane A. The control speakers 1–4 are mounted at the corner of the plane B. The measurement sensor is collocated with the primary source and four performance sensors are collocated with four control speakers. This configuration forms a 4 input/4 output system. The aforementioned

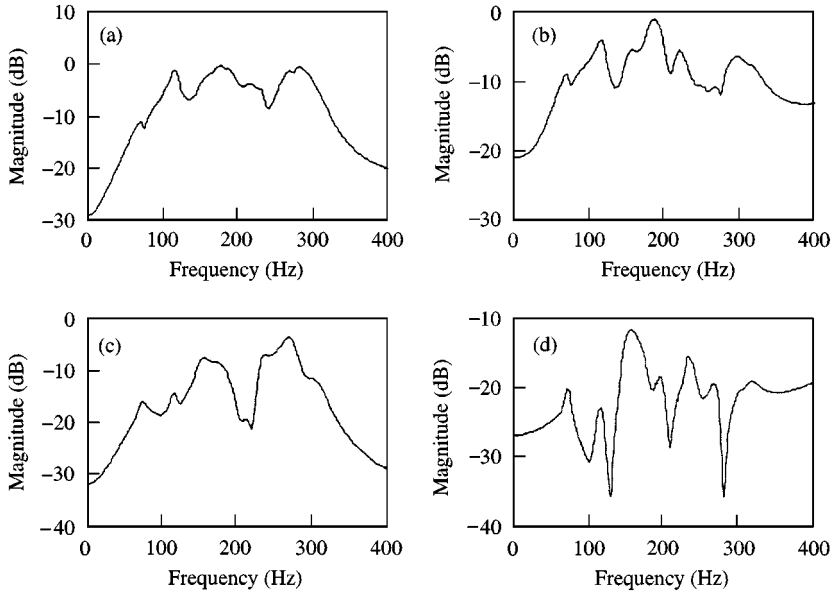

Figure 5. The models from the control speakers to the performance sensors and the measurement sensors identified by the frequency-domain procedure: (a) control speaker 3 to performance sensor 3; (b) control speaker 4 to performance sensor 4; (c) control speaker 3 to measurement sensor; (d) control speaker 4 to measurement sensor.

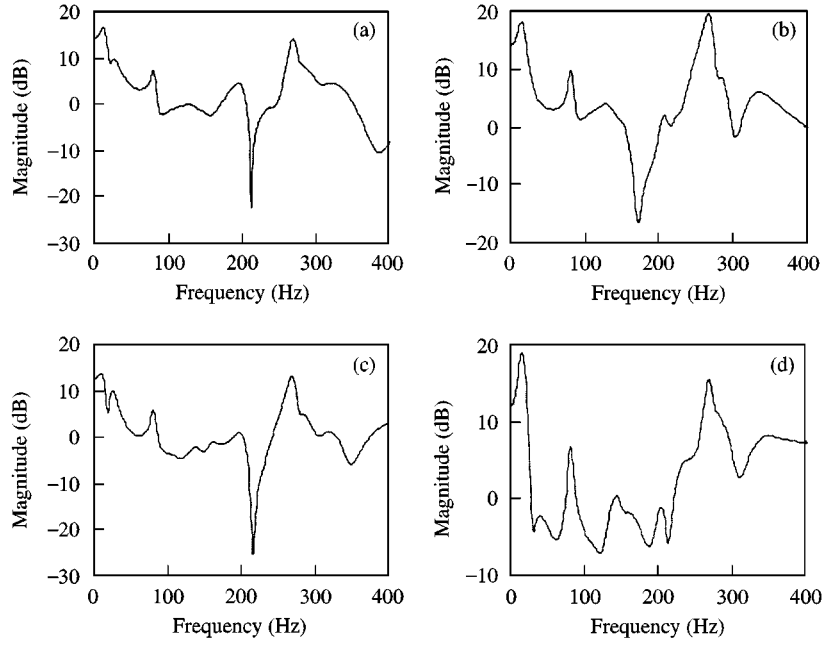

Figure 6. The controllers obtained by LQG synthesis (for the case of random noise): (a) for control speaker 1; (b)

frequency-domain procedure is used for identifying the plant model. A ZSP controller is designed via the LQG synthesis and is then implemented using a digital signal processor, TMS320C32. The sampling frequency is chosen to be 1 kHz. The control bandwidth covers

50–350 Hz because the speakers have poor frequency response below 50 Hz and the Schroeder's cut-off frequency is approximately 350 Hz.

Two types of noise are employed as the input to the primary source: a band-limited (0–512 Hz) random noise and an engine exhaust noise at 4000 r.p.m. In the first case, we assume that the disturbance input is measurable and the frequency response between voltage input to the primary source and each sensor output is known. In the second case, we assume the disturbance input is not measurable, as in many practical applications.

4.1. RANDOM NOISE

Figures 4(a)–4(d) are frequency response functions from the primary source to the performance sensors. Figures 5(a)–5(d) also show some examples of frequency response functions from the control speakers to the performance sensors and to the measurement sensor. The frequency-domain procedure is used for identifying the plant. Figures 6(a)–6(d) show the frequency responses of ZSP controller obtained by LQG synthesis. The results

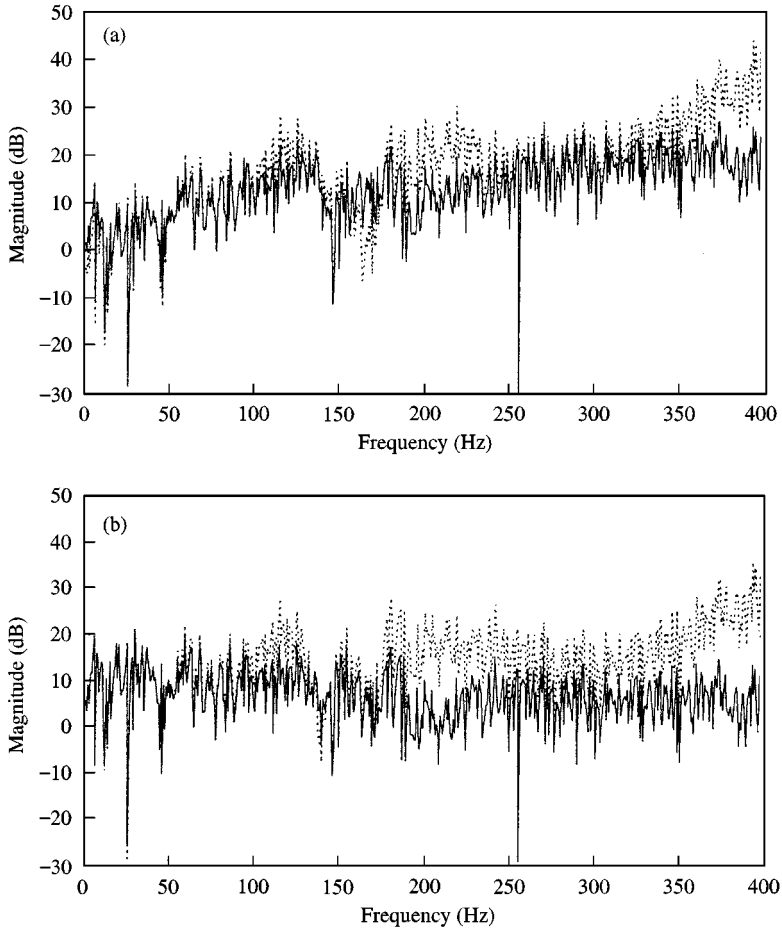

Figure 7. The power spectra for the case of random noise before and after ANC is activated: (a) performance sensor 1; (b) performance sensor 2; (c) performance sensor 3, (d) performance sensor 4.

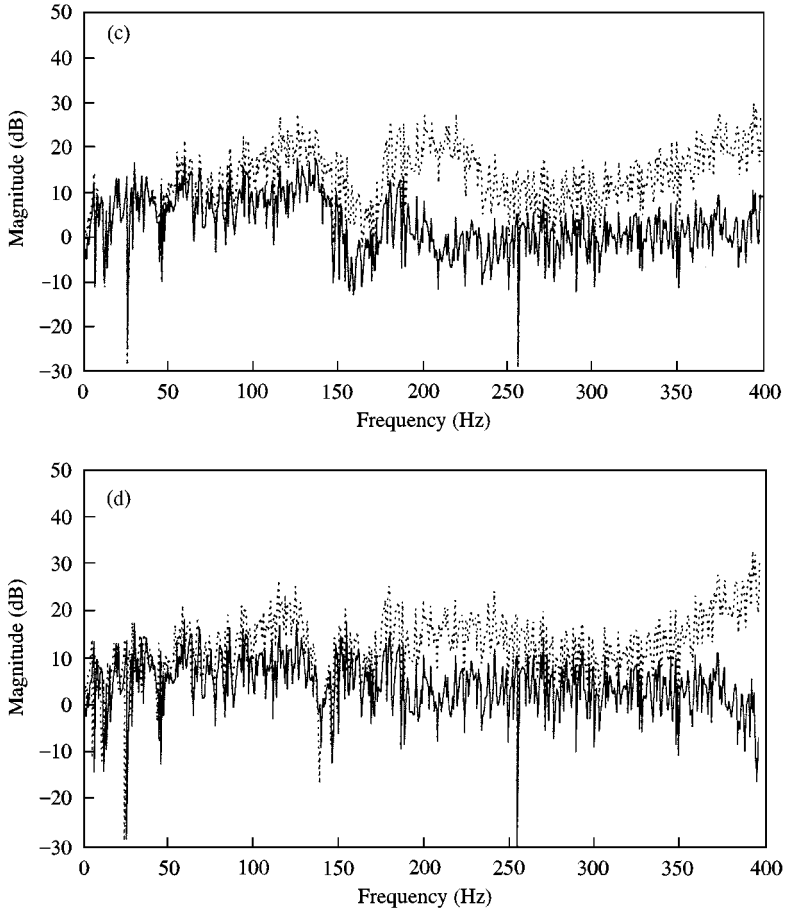

Figure 7. Continued.

before and after ANC is activated are shown in Figures 7(a)–7(d). From Figure 7(a) we see that the noise is attenuated in some regions within 100–400 Hz. In Figures 7(b)–7(d), the maximum attenuation reaches 25 dB. It appears that the ANC system is effective in a wide-band region, which is in general very difficult for problems of large size. Sensors 2 and 3 show better performance than the other sensors.

4.2. ENGINE EXHAUST NOISE

In practical applications such as engine noise and fan noise, the disturbance input to the system is hardly available. This poses a problem in the design of ZSP controller that requires the transfer functions between the primary source and the sensors. However, partial knowledge about the noise dynamics, e.g., the rotating speed, helps alleviate the problem. Control effort is thus focused on the peaks of the noise spectrum that are generally the fundamental and its multiples related to the shaft speed. To make use of the shaft speed information, the frequency response of $\mathbf{G}_{wy}(z)$ is assumed to be as shown in Figure 8(a),

where two peaks at 70 and 140 Hz can be observed. The disturbance model may have been constructed by more sophisticated methods, e.g., spectral factorization. However, we found that this simple approach seemed to be sufficient in our experiment. On the other hand, the frequency response functions between the measurement sensor and the performance sensors ($\mathbf{G}_{yz}(z)$) are also measured. For example, the frequency response from the measurement sensor to the performance sensor 4 is shown in Figure 8(b). Thus, the transfer function from the primary source to the performance sensors can be constructed as

$$\mathbf{G}_{wz}(z) = \mathbf{G}_{wy}(z)\mathbf{G}_{yz}(z).$$

For example, the frequency response from the primary source to the performance sensor 4 is shown in Figure 8(c). The frequency-domain procedure is used for identifying the plant. Figure 9 shows the ZSP controller designed by LQG synthesis. The results before and after ANC is activated are shown in Figures 10(a)–10(d). Note that signals in 70 and 140 Hz are significantly attenuated with a maximum 12 dB. Sensors 2,3 and 4 yield better performance sensor 1.

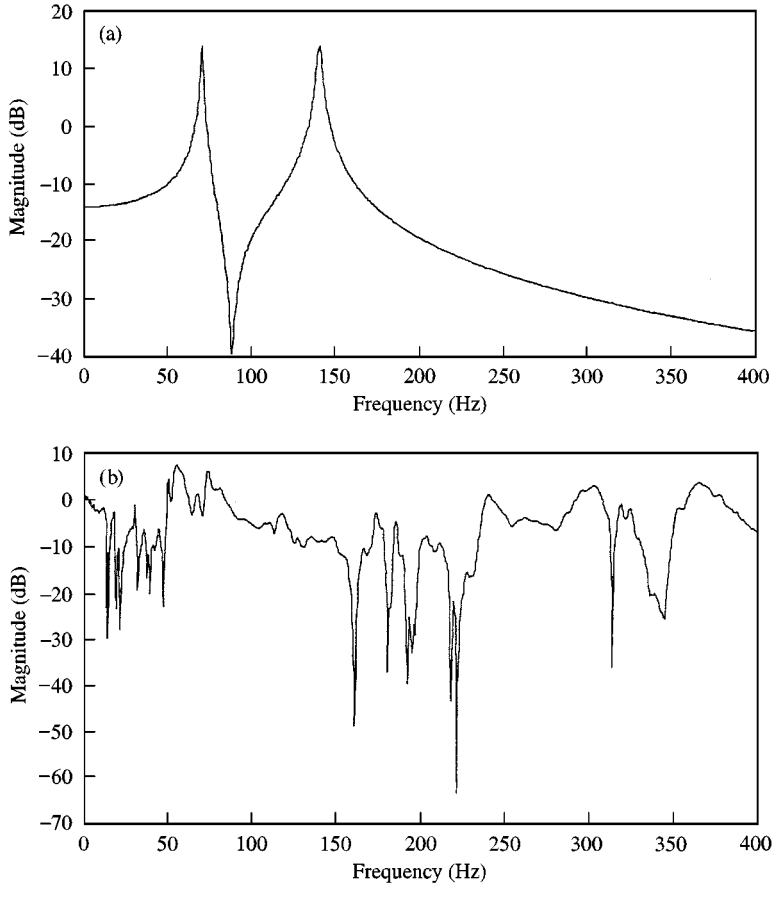

Figure 8. The frequency response functions involved in the case of the engine noise: (a) the assumed model from the primary source to the measurement sensor; (b) the measured frequency response from the measurement sensor to the performance sensor 4; (c) the overall frequency response from the primary source to performance sensor 4.

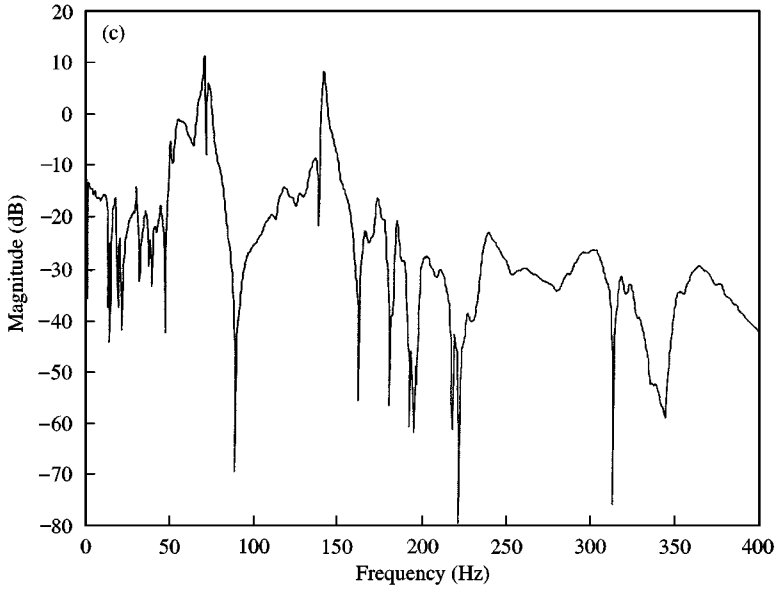

Figure 8. Continued.

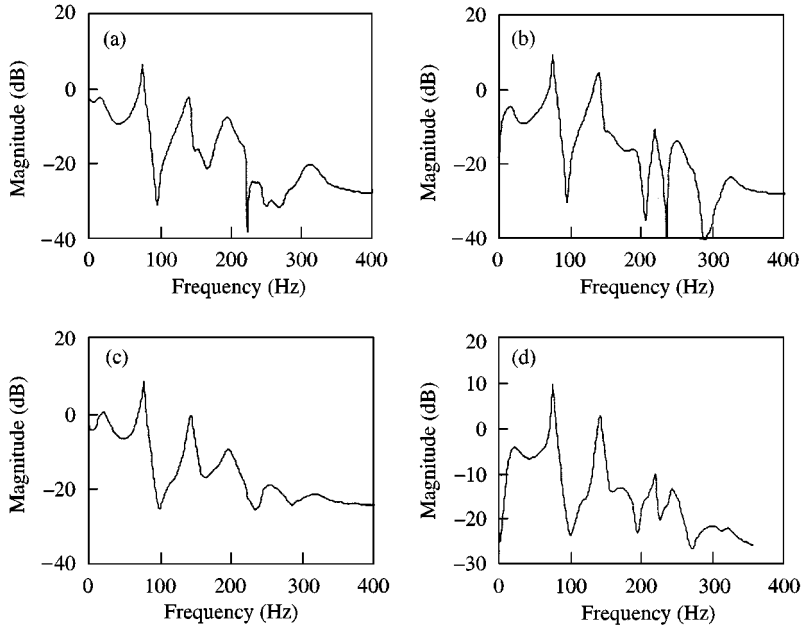

Figure 9. The controllers obtained by LQG synthesis (for the case of engine noise): (a) for control speaker 1; (b) for control speaker 2; (c) for control speaker 3; (d) for control speaker 4.

5. CONCLUSIONS

A multiple-channel ZSP controller using spatially feedforward structure is investigated. Random noise and engine noise are chosen as the primary noises. The experimental results

show the system produced significant reduction for the random noise when the disturbance input is measurable. The ZSP controller is also found to be effective in attenuating the engine noise when an assumed model of the disturbance is included in the controller design. However, the uncertainty plant model could be crucial in the resulting performance. This remains to be explored in the future research.

It has been widely believed that the adaptive feedforward scheme can be used as an effective alternative whenever the reference signal is obtainable such as the engine exhaust noise in our case. This is true under well-controlled laboratory conditions. However, our experience obtained from field tests showed that the adaptive algorithm could easily diverge for cases of usual engine slew rates or during gear shifting because the learning process of the adaptive algorithm failed to respond fast enough to the changing operation conditions. In our opinion, a more reliable and practical approach would be the "gain scheduling approach" which is simply a table lookup method of fixed controllers (including the assumed models) pre-designed for various operating speeds. Each fixed controller is robust within certain localized range of the operating speed. Many modern control methods such as $\mathbf{H}_\infty$ control, μ-synthesis and linear matrix inequality can be employed in designing robust controllers so that the plant uncertainties can be better dealt with. More research in the future will be done to support this claim.

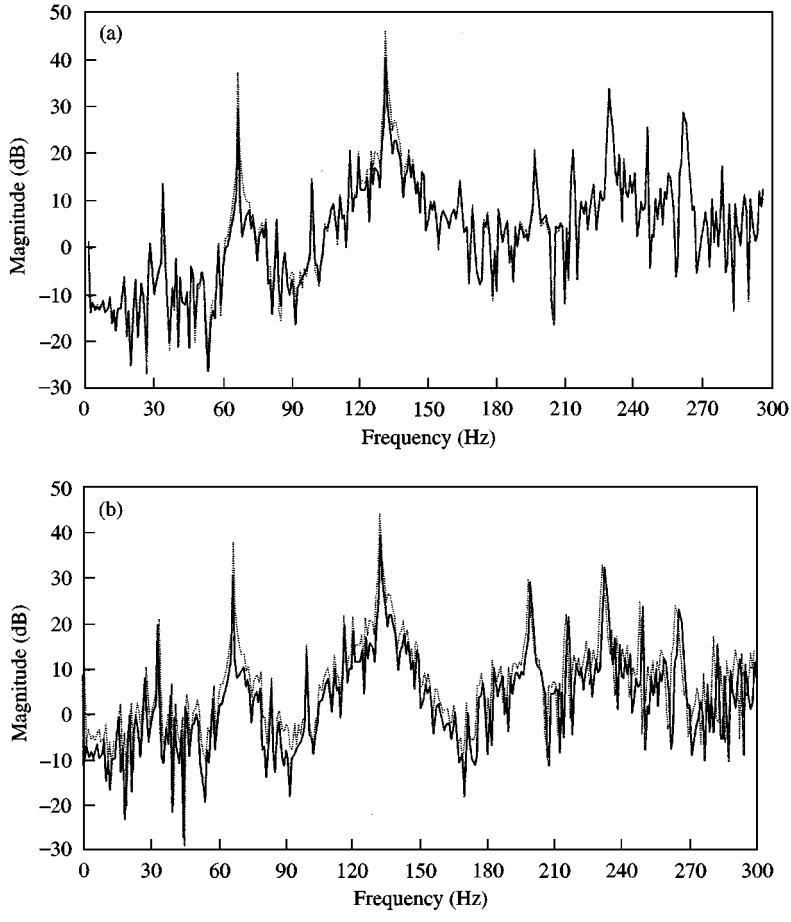

Figure 10. The power spectra for the case of engine noise before and after ANC is activated: (a) performance sensor 1; (b) performance sensor 2; (c) performance sensor 3; (d) performance sensor 4.

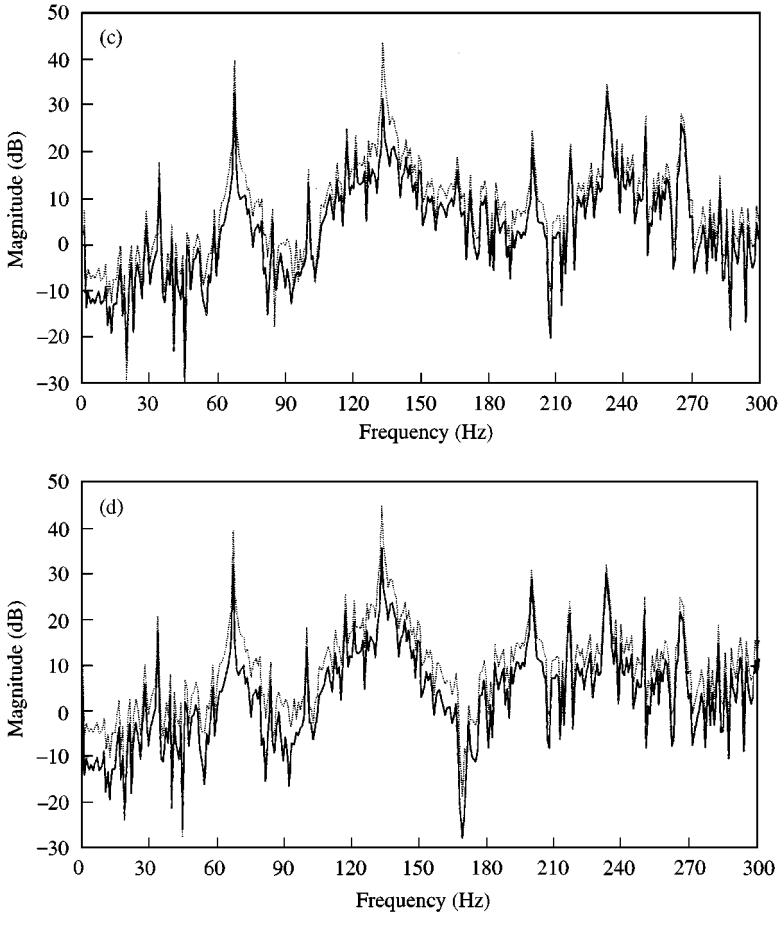

Figure 10. Continued.

ACKNOWLEDGMENTS

The work was supported by the National Science Council in Taiwan, Republic of China, under the project number NSC 87-2212-E009-022.

REFERENCES

1. S. M. KUO and O. R. MORGAN 1996 *Active Noise Control Systems.* New York: Wiley Interscience.
2. M. R. BAI and D. J. LEE 1997 *Journal of the Acoustical Society of America* **102**, 2184–2190. Implementation of an active headset by using the H_∞ robust control theory.
3. M. R. BAI and Z. LIN 1998 *ASME, Journal of Vibration Acoustics* **120**, 958–964. Active noise cancellation for a three-dimensional enclosure by using multiple-channel adaptive control and H_∞ control.
4. J. HONG and D. S. BERNSTEIN 1998 *IEEE Transactions on Control System Technology* **6**, 111–120. Bode integral constraints, collocation, and spillover in active noise and vibration control.
5. J. JUANG 1994 *Applied System Identification.* Englewood Cliffs, NJ: Prentice-Hall.
6. F. L. LEWIS and V. L. SYRMOS 1995 *Optimal Control.* New York: John Wiley & Sons.
7. F. L. LEWIS 1992 *Applied Optimal Control and Estimation.* Englewood Cliffs, NJ: Prentice-Hall.